MOLECULAR AND CELLULAR BIOLOGY, Aug. 1998, p. 4629–4638 Vol. 18, No. 8
0270-7306/98/$04.00+0

Disruption of Higher-Order Folding by Core Histone Acetylation Dramatically Enhances Transcription of Nucleosomal Arrays by RNA Polymerase III

CHRISTIN TSE,[1] TAKASHI SERA,[2] ALAN P. WOLFFE,[2] AND JEFFREY C. HANSEN[1]*

Department of Biochemistry, The University of Texas Health Science Center at San Antonio, San Antonio, Texas 78284-7760,[1] and Laboratory of Molecular Embryology, National Institute of Child Health and Human Development, National Institutes of Health, Bethesda, Maryland 20892-5431[2]

Received 3 April 1998/Returned for modification 18 May 1998/Accepted 20 May 1998

We have examined the effects of core histone acetylation on the transcriptional activity and higher-order folding of defined 12-mer nucleosomal arrays. Purified HeLa core histone octamers containing an average of 2, 6, or 12 acetates per octamer (8, 23, or 46% maximal site occupancy, respectively) were assembled onto a DNA template consisting of 12 tandem repeats of a 208-bp *Lytechinus* 5S rRNA gene fragment. Reconstituted nucleosomal arrays were transcribed in a *Xenopus* oocyte nuclear extract and analyzed by analytical hydrodynamic and electrophoretic approaches to determine the extent of array compaction. Results indicated that in buffer containing 5 mM free Mg^{2+} and 50 mM KCl, high levels of acetylation (12 acetates/octamer) completely inhibited higher-order folding and concurrently led to a 15-fold enhancement of transcription by RNA polymerase III. The molecular mechanisms underlying the acetylation effects on chromatin condensation were investigated by analyzing the ability of differentially acetylated nucleosomal arrays to fold and oligomerize. In $MgCl_2$-containing buffer the folding of 12-mer nucleosomal arrays containing an average of two or six acetates per histone octamer was indistinguishable, while a level of 12 acetates per octamer completely disrupted the ability of nucleosomal arrays to form higher-order folded structures at all ionic conditions tested. In contrast, there was a linear relationship between the extent of histone octamer acetylation and the extent of disruption of Mg^{2+}-dependent oligomerization. These results have yielded new insight into the molecular basis of acetylation effects on both transcription and higher-order compaction of nucleosomal arrays.

The packaging of eukaryotic DNA into chromatin presents a major obstacle to the transcriptional machinery (reviewed in references 61 and 67). Acetylation of the core histone N termini is a post-translational modification of chromatin that has been widely correlated with enhanced transcriptional activity in vivo (3, 34, 55, 57). Understanding of the connection between histone acetylation and transcriptional regulation has been further strengthened by the recent demonstrations that transcriptional coactivators possess histone acetyltransferase activity (11) and that transcriptional repressors associate with histone deacetylases (52). Despite this strong correlative evidence, the mechanism(s) through which histone acetylation influences transcription remains speculative. At the nucleosome level, the decreased access of transcription factors to regulatory DNA elements in vitro due to wrapping of the DNA around the histone octamer in some cases can be relieved by acetylation of the core histone N termini (38, 63; reviewed in reference 44). Beyond the level of the nucleosome, histone acetylation may function by disrupting higher-order folding of nucleosomal arrays. Studies of selectively trypsinized nucleosomal arrays have established that the core histone N termini perform multiple essential functions during nucleosomal array condensation (1, 17, 21, 54). While this makes disruption of higher-order folding an attractive potential candidate for a targeted site of histone acetylation, very little is actually known about the folding properties of acetylated nucleosomal arrays. When linker histones are present, high levels of acetylation at best have modest effects on the destabilization of higher-order folding (4, 40). When linker histones are absent from nucleosomal arrays, acetylation inhibits the intermediate level of array folding that occurs in NaCl (22). However, the effect of acetylation on the higher-order transcriptionally repressive structures (30, 48) formed in physiologically relevant buffers containing Mg^{2+} has yet to be determined. Although functional studies have shown that core histone acetylation enhances transcription initiation and elongation by RNA polymerase III from dinucleosomal templates (58), the role of folding in these experiments is equivocal because a dinucleosome cannot reproduce all of the internucleosomal interactions that lead to formation of higher-order chromatin structures (8, 60, 70, 71).

To directly determine whether changes in higher-order structure due to acetylation were correlated with altered transcriptional activity, as well as to better understand the mechanisms through which histone acetylation mediates higher-order folding of nucleosomal arrays, we have made use of a 12-mer nucleosomal array model system in which histone octamers are reconstituted onto a DNA template composed of 12 tandemly repeated functional *Lytechinus* 5S rRNA gene segments (27, 30, 51). Each 5S ribosomal DNA (rDNA) repeat specifically positions a single nucleosome, and the positioning is unaffected by the absence of the core histone N termini (16, 41). Consequently, this system is ideal for the analysis of the roles of the core histone N termini in nucleosomal array condensation (17, 21, 47, 54). In addition, because each 5S rDNA repeat can be efficiently transcribed by RNA polymerase III in vitro (30, 31), this system also permits determination of direct correlations between higher-order folding and transcriptional activity. In the present work, we explored the relationships

* Corresponding author. Mailing address: Department of Biochemistry, The University of Texas Health Science Center at San Antonio, 7703 Floyd Curl Dr., San Antonio, TX 78284-7760. Phone: (210) 567-6980. Fax: (210) 567-6595. E-mail: hansen@bioc02.uthscsa.edu.

among histone acetylation, transcription, and higher-order compaction of the 5S nucleosomal arrays. Purified fractions containing three different levels of acetylated histone octamers (corresponding to 8, 23, and 46% maximal site occupancies) have been reconstituted onto the tandemly repeated 12-mer 5S rDNA template. The resulting nucleosomal arrays were transcribed in *Xenopus* oocyte nuclear extracts and characterized by quantitative hydrodynamic and electrophoretic assays to establish the degree of folding under identical ionic conditions. Results indicated that above a critical level, acetylation disrupted each of the steps involved in the formation of highly condensed nucleosomal arrays. In addition, inhibition of higher-order folding by acetylation was correlated with a large enhancement in the ability of RNA polymerase III to transcribe through the 12-mer nucleosomal arrays. These results both suggest that disruption of higher-order folding by acetylation provides a key mechanism for regulating the transcriptional activity of nucleosomal arrays and provide new insight into the mechanistic basis of core histone acetylation effects on chromatin fiber condensation.

MATERIALS AND METHODS

Materials. HeLa cells (S3 strain) were acquired from the American Type Culture Collection. Fetal bovine serum and media were obtained from Gibco/BRL. Whole chicken blood was purchased from Pel-Freeze. Milligram quantities of DNA templates consisting of 12 tandem repeats of a 208-bp sequence derived from the *Lytechinus* 5S rRNA gene (208-12 DNA) were grown and purified from plasmid pPOL208-12 (23) by using a modified alkaline lysis protocol followed by *Hha*I digestion and exclusion chromatography as described previously (48). All chemicals were of reagent grade.

Purification of differentially acetylated histone octamers from HeLa cells. HeLa cells were grown in suspension at 37°C in Joklik's modified medium plus 10% fetal bovine serum and harvested when the cell density reached $\sim 5 \times 10^5$ cells/ml. To inhibit histone deacetylases, cells were treated with 10 mM sodium butyrate for 22 to 24 h prior to harvesting. Chromatin fractions varying in their degree of core histone octamer acetylation were isolated based on differential salt solubility essentially as previously described (5), with the exception that we found it necessary to also include 2.5 mM dithiothreitol (DTT) in buffers to prevent H3-H3 cross-linking during octamer purification and reconstitution into nucleosomal arrays. Briefly, suspended cells were harvested by centrifugation at 4°C for 10 min at $1,000 \times g$, resuspended in buffer A (10 mM morpholineethanesulfonic acid [MES], 0.25 M sucrose, 5 mM $MgCl_2$, 60 mM KCl, 15 mM NaCl, 1 mM $CaCl_2$, 10 mM sodium butyrate, 0.5% Triton X-100, 0.1 mM phenylmethylsulfonyl fluoride (PMSF) [pH 6.5]), and centrifuged at $3,000 \times g$ for 10 min at 4°C. The cell pellet was resuspended and centrifuged at $3,000 \times g$ for 10 min at 4°C in buffer A two additional times to yield purified HeLa nuclei. Pelleted nuclei were resuspended to an A_{260} of ~40 in buffer B {10 mM PIPES [piperazine-*N*,N′ bis(2-ethanesulfonic acid)], 5 mM $MgCl_2$, 1 mM $CaCl_2$, 10 mM sodium butyrate, 0.1 mM PMSF, 2.5 mM DTT [pH 6.8]} containing 75 mM NaCl and were digested with 20 U of micrococcal nuclease per mg of chromatin for 4 min at 37°C. The micrococcal nuclease reaction was quenched by addition of EDTA to a final concentration of 5 mM, and the digested nuclei were centrifuged at $5,000 \times g$ for 5 min at 4°C. The supernatant containing the most highly acetylated chromatin was collected and is referred to throughout as fraction A. The pellet subsequently was resuspended in buffer B containing 175 mM NaCl and incubated for 15 min on ice. After centrifugation at $5,000 \times g$ for 5 min at 4°C, the supernatant (fraction B) was collected and discarded. The pellet was then resuspended in buffer C (10 mM Tris–HCl, 2 mM EDTA, 5 mM $MgCl_2$, 350 mM NaCl, 10 mM sodium butyrate, 2.5 mM DTT, 0.2 mM PMSF [pH 7.5]) and incubated on ice for 15 min. After centrifugation at $5,000 \times g$ for 5 min at 4°C, the supernatant, which contained moderately acetylated chromatin, was collected, and it is referred to as fraction C. As a control, underacetylated chromatin was isolated from untreated HeLa cells. Briefly, untreated cells were harvested by centrifugation at 4°C for 10 min at $1,000 \times g$. The harvested cells were washed three times in buffer A in the same fashion as the butyrate-treated cells. The resulting nuclei pellet was resuspended to an A_{260} of ~40 in buffer B containing 75 mM NaCl and was digested with 20 U of micrococcal nuclease per mg of chromatin for 4 min at 37°C. The nuclease reaction was quenched by the addition of EDTA to a final concentration of 5 mM, and the digested nuclei were centrifuged at $5,000 \times g$ for 5 min at 4°C. The supernatant was discarded, and the pelleted nuclei were resuspended in lysis buffer (1 mM EDTA, 10 mM sodium butyrate, 2.5 mM DTT, 0.2 mM PMSF [pH 7.5]) and gently stirred for 30 min at 4°C. The resuspended nuclei were centrifuged at $5,000 \times g$ for 5 min at 4°C. The supernatant was collected and contained the least-acetylated chromatin fragments. Chicken erythrocyte chromatin was isolated as described previously (48).

Histone octamers were purified by first dialyzing the various chromatin fractions against buffer C overnight at 4°C. Linker histones and other nonhistone-associated proteins were removed from the chromatin fragments by incubation with 20 mg of carboxymethyl-Sephadex per mg of chromatin with gentle stirring for 3 h at 4°C, followed by centrifugation at $6,500 \times g$ for 30 min at 4°C. After collection of the supernatant, core histone octamers were purified from the stripped oligonucleosomes by hydroxylapatite chromatography as described previously (50), except that the elution buffer also contained 5 mM sodium butyrate and 2.5 mM DTT. Purified histone octamers were quantitated by measuring the absorbance at 230 nm and were stored at a concentration of ~0.40 μg/μl in elution buffer at 4°C.

Reconstitution of nucleosomal arrays. Nucleosomal arrays were reconstituted from the various histone octamer fractions and 208-12 DNA by using the salt dialysis protocol described by Hansen and Lohr (29) with several minor modifications. All reconstitution buffers contained 10 mM Tris–HCl, 0.25 mM EDTA, 2.5 mM sodium butyrate, 2.5 mM DTT, and various concentrations of NaCl. The ratio of moles of histone octamer to moles of 208-bp DNA was 1.2. The 208-12 DNA concentration was ~100 μg/ml. After combination of the histone octamer fractions and DNA, the NaCl concentration initially was 2 M. Samples subsequently were dialyzed against 2.0 liters of reconstitution buffer containing the indicated NaCl concentration as follows: 1.0 M NaCl, 4 h; 0.75 M NaCl, 3 h; 2.5 mM NaCl, 3.5 h. The final dialysis was overnight at 4°C against 10 mM Tris–HCl–0.25 mM EDTA–2.5 mM sodium butyrate–2.5 mM DTT (pH 7.8) (TE). Reconstitutes were stored at 4°C until used.

Analytical ultracentrifugation. Sedimentation velocity experiments were performed with a Beckman XL-A analytical ultracentrifuge equipped with absorption optics as previously described (48). The A_{260} of the samples was between 0.6 and 0.8. The integral distribution of sedimentation coefficients was determined by the method of van Holde and Weischet (62) with Ultrascan data analysis software version 2.95.

Quantitative agarose gel electrophoresis. Electrophoretic mobilities (μ) of nucleosomal arrays in 0.2 to 3.0% agarose running gels were determined by using an 18-lane multigel apparatus as previously described (19, 28). Running gels were cast in E buffer (40 mM Tris-HCl–0.25 mM EDTA [pH 7.8]) containing either 0 or 2 M free Mg^{2+}. Samples containing nucleosomal arrays and an added bacteriophage T3 standard were dialyzed against running buffer for ≥3 h at 4°C prior to electrophoresis. Samples were electrophoresed at 1 V/cm for 8 h and were visualized by UV illumination after ethidium bromide staining. The gel-free μ (μ'_0) was determined by extrapolation of the linear region of a plot of log μ versus agarose concentration to 0% agarose by using a standard linear regression. The linear region generally corresponded to 0.2 to 0.5% agarose for both the nucleosomal arrays and T3 phage, and the extrapolations yielded a correlation coefficient of 0.99 (see Fig. 2D). The nucleosomal array μ'_0 was subsequently corrected for electroosmosis and normalized to yield the μ_0 as previously described (19). The pore size, P_e, of each running gel was calculated from the experimentally determined μ, μ'_0, and known effective radius (R_e) of the bacteriophage T3 standard (30.1 nm) by using the equation $\mu/\mu'_0 = (1 - R_e/P_e)^2$ (19, 24, 28). The R_e of each nucleosomal array was calculated from the experimentally determined μ, μ'_0, and P_e with the same equation (19, 28).

In vitro transcription. Transcription buffer consisted of 10 mM Na–HEPES–2.5 mM DTT–0.1 mM Na_2EDTA–5% glycerol–50 mM KCl–7 mM $MgCl_2$ (pH 7.4). The free Mg^{2+} concentration in transcription buffer was 5 mM after the addition of 2 mM nucleoside triphosphates (see below) (30). Nuclear extracts were prepared from *X. laevis* oocytes as described previously (9, 66). Transcription reactions were conducted in transcription buffer in the following fashion. Reconstitutes (120 ng in 5 μl of TE buffer) were mixed with 5 μl of a 4× stock solution of transcription buffer containing 0.25 U of RNasin (Gibco/BRL)/μl. Ten microliters of nuclear extract was subsequently added, and the samples were incubated at room temperature for 30 min. Transcription was initiated by the addition of 0.5 mM (each) ATP, GTP, CTP, and UTP. The latter consisted of 0.1 mM unlabeled UTP and 0.4 mM [^{32}P]UTP (5 μCi). After 90 min at room temperature, the reactions were quenched by the addition of 20 μl of 15 mM Tris–HCl–7.5 mM EDTA–1% sodium dodecyl sulfate (SDS) (pH 8.0) containing 10 to 15 μg of proteinase K. The RNA transcripts were purified by phenol-chloroform extraction, precipitated with ethanol, and resuspended in formamide loading buffer prior to resolution by electrophoresis on a 9% polyacrylamide gel as previously described (30).

RESULTS

Assembly of differentially acetylated nucleosomal arrays. Core histone octamers containing different levels of acetylation were obtained from butyrate-treated HeLa oligonucleosomes that were soluble in either 5 mM $MgCl_2$–350 mM NaCl (fraction C, see Materials and Methods) or 5 mM $MgCl_2$–75 mM NaCl (fraction A). Histone octamers purified from untreated HeLa cells and chicken erythrocytes served as controls. SDS-polyacrylamide gel electrophoresis of the purified histones is shown in Fig. 1A. The extent of histone acetylation in each fraction was determined by Triton X-100-urea-acetic acid poly-

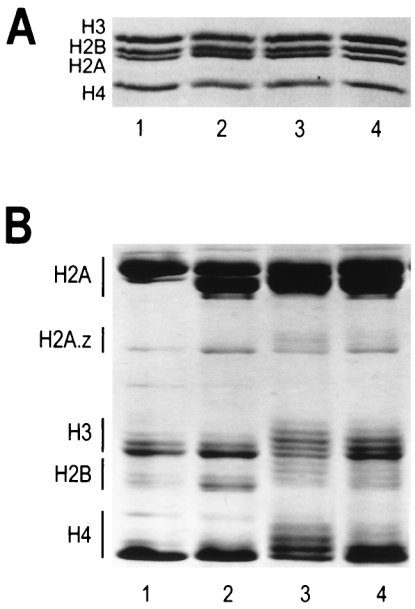

FIG. 1. Analysis of core histone octamers purified from HeLa cells and chicken erythrocytes. (A) SDS-polyacrylamide gel electrophoresis. Two micrograms of purified histone octamers were electrophoresed on an SDS–18% polyacrylamide gel (37), and bands were visualized by staining with Coomassie blue G-250. Samples were loaded as follows: lane 1, chicken erythrocyte octamers; lane 2, underacetylated octamers isolated from untreated HeLa cells; lane 3, highly acetylated octamers isolated from fraction A of butyrate-treated HeLa cells (see Materials and Methods); lane 4, moderately acetylated octamers isolated from fraction C of butyrate-treated HeLa cells. (B) Resolution of acetylated histone species. Fifteen micrograms of the histone octamers from panel A were electrophoresed on a 6 M acetic acid–6 M urea–0.375% Triton X-100–polyacrylamide gel (12) for 16 h at 5 mA of constant current. The bands were visualized by Coomassie blue G-250 staining. Lanes 1 to 4 correspond to the same histone octamers as in panel A. Histones H2B, H3, and H4 each have four acetylation sites, while H2A has only one acetylation site (53). For each core histone (with the exception of H2A), increasing extents of acetylation lead to progressively slower band migration. In the case of histone H2A, the slower-migrating band corresponds to H2A.1 while the faster-migrating band corresponds to the H2A.2 variant (65).

acrylamide gel electrophoresis (Fig. 1B). Densitometric quantitation indicated an average of approximately two acetyl groups per histone octamer purified from untreated cells, while histone octamers isolated from fractions A and C had weighted averages of 12 and 6 acetyl groups, respectively. Octamers containing an average of 2, 6, or 12 acetates (corresponding to 8, 23, or 46% maximum site occupancy) are referred to throughout as underacetylated, moderately acetylated, or highly acetylated, respectively. For each octamer fraction, the distribution of acetylated core histone species is summarized in Table 1. The additional four acetates present in moderately acetylated octamers resulted from increased amounts of diacetylated H2B and H3 and monoacetylated H4. The additional six acetyl groups present in the highly acetylated octamers primarily reflected increased amounts of triacetylated H2B, tri- and tetraacetylated H3, and di-, tri- and tetraacetylated H4 (Table 1). The amounts of unacetylated and monoacetylated histone H2A in each fraction could not be determined since these species did not separate into discrete bands. Consistent with previous results (65), histone octamers isolated from both untreated and sodium butyrate-treated HeLa cells had equivalent amounts of the H2A.1 and H2A.2 variants whereas chicken erythrocyte octamers contained mainly H2A.1 (Fig. 1B).

Underacetylated, moderately acetylated, and highly acetylated 12-mer nucleosomal arrays were assembled from the histone octamer fractions shown in Fig. 1 and the 208-12 DNA template (Fig. 2A) by using a simplified salt dialysis protocol (29, 54). Reconstitutes initially were characterized by micrococcal nuclease digestion. Irrespective of the degree of acetylation, mild digestion conditions produced ladders of 12 regularly spaced bands (Fig. 2B). Extensive digestion of all three nucleosomal array preparations yielded a well-defined ~147-bp core particle band (data not shown). Because only fully saturated 208-12 templates containing 12 histone octamers are capable of higher-order folding (20, 29, 48) (see Fig. 3D and 4) it was essential for the sake of the comparative folding studies described below to document that the underacetylated, moderately acetylated, and highly acetylated nucleosomal array preparations were equally saturated with histone octamers after reconstitution. Octamer saturation was determined by using an *Eco*RI digestion assay. Flanking each 208-bp 5S repeat are two *Eco*RI restriction sites (51) (Fig. 2A). *Eco*RI digestion of 5S nucleosomal arrays yields a mixture of histone-free 5S rDNA repeats, mononucleosomes, and a fraction of partially digested arrays that results from heterogeneity in nucleosome positioning (16, 27, 41, 54). After resolution of the digestion products by gel electrophoresis and subsequent densitometric quantitation, the ratio of the naked 5S rDNA band to nucleosomal bands provided a sensitive measure of the overall extent of DNA template saturation (54). The products obtained after *Eco*RI digestion of each of the reconstitutes are shown in Fig. 2C. The amounts of naked 5S rDNA repeats liberated from the underacetylated, moderately acetylated, and highly acetylated nucleosomal arrays constituted 3.9% ± 1.3%, 3.6% ± 1.1%, and 4.0% ± 1.3% of the total digestion products, respectively. Importantly, these results indicated both that the differentially acetylated reconstitutes were equally saturated and that in each case ~50% of the DNA templates contained 12 histone

TABLE 1. Quantitation of the extent of acetylation of the individual core histones

No. of acetyl groups/histone	Avg % of total acetates (by wt) for each histone[a]:											
	H2A			H2B			H3			H4		
	U	M	H	U	M	H	U	M	H	U	M	H
0	nd[b]	nd	nd	73	41	16	66	43	20	98	51	24
1	nd	nd	nd	27	32	21	27	23	21	nd	35	33
2				nd	27	28	7	22	28	nd	9	24
3				nd	nd	35	nd	9	21	nd	5	15
4				nd	nd	nd	nd	3	10	2	nd	5

[a] U, underacetylated octamer; M, moderately acetylated octamer; H, highly acetylated octamer.
[b] nd, not detected.

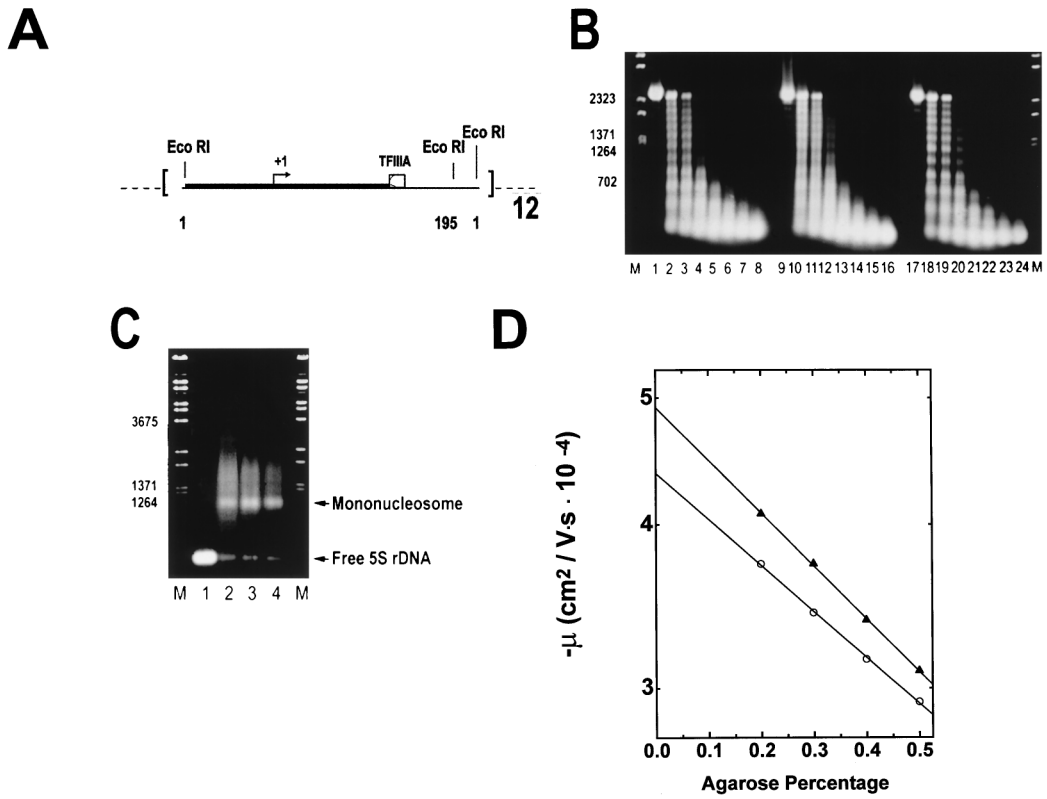

FIG. 2. Reconstitution of underacetylated, moderately acetylated, and highly acetylated 208-12 nucleosomal arrays. (A) Schematic illustration of the 208-12 DNA template used for reconstitution. The 208-12 DNA consists of 12 tandem repeats of a portion of the *Lytechinus* 5S rRNA gene (51). Each 5S rDNA repeat contains both a preferred nucleosome positioning site (solid box) and a TFIIIA binding site (open box). Initiation of transcription by RNA polymerase III occurs ~90 bp upstream of the major TFIIIA binding site (+1, arrow). The termination sequence of the 5S rRNA gene was deleted during template construction (51), allowing for production of long read-through transcripts. *Eco*RI digestion sites are located at sequences 1 and 195 of each 5S rDNA repeat. (B) Micrococcal nuclease digestion. Underacetylated (lanes 1 to 8), highly acetylated (lanes 9 to 16), and moderately acetylated (lanes 17 to 24) reconstitutes were digested with 0.05 U of micrococcal nuclease per μg of DNA in the presence of 1 mM $CaCl_2$. Digestion was for 0, 0.5, 1.0, 2.5, 5, 10, 20, and 30 min (shown from left to right for each reconstitute type) at room temperature. The reactions were quenched by addition of a 1/5 volume of 5% SDS–25% glycerol–10 mM EDTA–0.3% bromophenol blue. Samples were deproteinated by incubation at 37°C for 30 min and subsequently electrophoresed for 5 h at 2 V/cm in a 1% agarose gel buffered with 40 mM Tris-acetate–1 mM EDTA (pH 8.0). Bands were visualized under UV illumination after incubation of the gel in ethidium bromide. Lambda DNA digested with *Bst*EII (lanes M) was used for the size markers. (C) *Eco*RI digestion. One microgram (each) of naked 208-12 DNA (lane 1) and underacetylated, highly acetylated, and moderately acetylated nucleosomal arrays (lanes 2 to 4, respectively) was digested with 10 U of *Eco*RI for 60 min at room temperature in digestion buffer H (Promega). Reactions were quenched by addition of a 1/5 volume of 25% glycerol–10 mM EDTA (pH 8.0). Digestion products were electrophoresed at 4 V/cm for 3 h in a 1% agarose gel buffered with 40 mM Tris-acetate–1 mM EDTA (pH 8.0). Lambda DNA digested with *Bst*EII (lanes M) was used for the size markers. (D) Determination of μ_0. Shown are plots of the mobilities in 0.2 to 0.5% agarose of underacetylated (○) and highly acetylated (▲) nucleosomal arrays in E buffer. The μ_0 was determined from the extrapolated gel-free mobilities as described in Materials and Methods.

octamers with the remainder containing 10 to 11 octamers (54).

To determine the average extent of array acetylation after reconstitution, we measured the μ_0 under low-salt conditions by using quantitative agarose gel electrophoresis in a multigel (19, 28). The value of the μ_0 is directly proportional to the macromolecular surface charge density (49) and therefore should be sensitive to the degree of acetylation. The μ_0 is obtained experimentally by extrapolating the linear region of a plot of log mobility versus agarose percentage to 0% agarose (Fig. 2D) (19, 28). Low-salt E buffer was used in these experiments to avoid contributions to the μ_0 term arising from Mg^{2+}-DNA interactions and nucleosomal array folding (20). Representative plots of log mobility versus agarose percentage for underacetylated and highly acetylated nucleosomal arrays are shown in Fig. 2D. It should be noted that for moderately acetylated arrays, the mobility extrapolated to 0% agarose fell between that of the underacetylated and highly acetylated arrays in three separate experiments (data not shown). From these experiments, the μ_0s of underacetylated, moderately acetylated, and highly acetylated nucleosomal arrays in E buffer were calculated to be $-1.91 \times 10^{-4} \pm 0.01 \times 10^{-4}$, $-1.94 \times 10^{-4} \pm 0.03 \times 10^{-4}$, and $-1.99 \times 10^{-4} \pm 0.03 \times 10^{-4}$ $cm^2/V \cdot s$, respectively. The μ_0 of 208-12 nucleosomal arrays containing 12 chicken erythrocyte chicken octamers was $-1.92 \times 10^{-4} \pm 0.02 \times 10^{-4}$ $cm^2/V \cdot s$ (19, 20). Given that the different preparations of acetylated reconstitutes were equivalently saturated with histone octamers (Fig. 2C), the magnitudes of the decreases in the μ_0s of the moderately acetylated and highly acetylated nucleosomal arrays correspond to neutralization by acetylation of ~6 and ~13 positive charges per nucleosome, respectively. This is in very close agreement with the value determined from Triton X-100-urea-acetic acid gel analysis of the purified histone octamers (Fig. 1B) and is the expected result if ≥50% of templates were saturated with histone octamers. Importantly, the data in Fig. 1 and 2 and Table 1 rigorously establish that the various nucleosomal arrays preparations used in our studies were sufficiently saturated to form higher-order folded structures and differed only in their average extent of histone octamer acetylation.

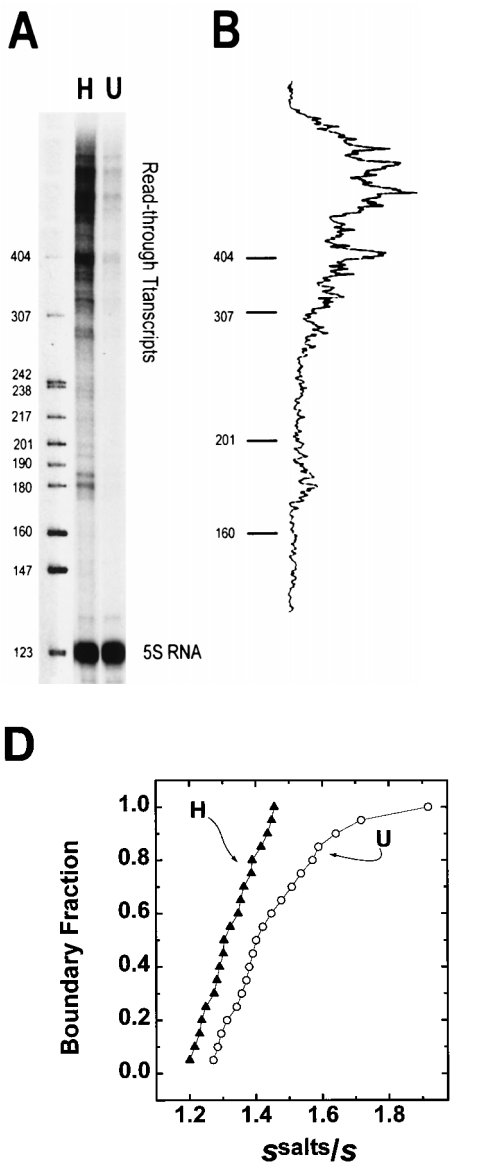

FIG. 3. Highly acetylated histones enhance transcription and disrupt folding of 208-12 nucleosomal arrays in transcription buffer. (A) In vitro transcription. Underacetylated (U) and highly acetylated (H) nucleosomal arrays were transcribed in *Xenopus* oocyte nuclear extracts as described in Materials and Methods. A histone-free plasmid containing one copy of the *Xenopus* 5S RNA gene (which produces a 120-nt transcript) was included in each reaction as an internal control. Transcription reactions were electrophoresed in a denaturing 9% polyacrylamide gel. After electrophoresis, RNA products were visualized with a Molecular Dynamics PhosphorImager. *Msp*I-digested pBR322 was utilized as the size marker. (B) Densitometric trace of the RNA transcripts produced from the highly acetylated arrays shown in panel A. (C) Densitometric quantitation of the total amount of RNA transcripts produced from the highly acetylated nucleosomal arrays (solid bar) expressed as the fold increase over the underacetylated controls. Also shown is the fold increase previously reported by Ura et al. (58) for hyperacetylated dinucleosomes (open bar). (D) Sedimentation velocity analysis of nucleosomal array folding in transcription buffer. Highly acetylated (▲) and underacetylated (○) nucleosomal arrays were incubated in either transcription buffer or transcription buffer containing 50 mM KCl and 7 mM $MgCl_2$ for 1 h at room temperature. For these experiments, the nucleoside triphosphates in transcription buffer were replaced with 2 mM Na_5PPP_i to avoid interference with the absorbance optical system of the analytical ultracentrifuge as previously described (30, 31). Samples were sedimented at 18,000 rpm in an An-Ti60 rotor, and 20 boundary scans were collected. The temperature of the run was 21°C. Each boundary was divided into 20 equal fractions. The diffusion-corrected sedimentation coefficient at each boundary division was determined by the method of van Holde and Weischet (62), and the data were plotted as boundary fraction versus $s_{20,w}$ to yield the integral distribution of sedimentation coefficients present in the sample. For both highly acetylated and underacetylated samples, at each boundary fraction the data are expressed as the ratios of the $s_{20,w}$ in transcription buffer containing 50 mM KCl and 7 mM $MgCl_2$ divided by the $s_{20,w}$ in transcription buffer lacking salts (s^{salts}/s) to yield the salt-dependent increase in $s_{20,w}$ across the entire distribution (30, 31). The s^{salts}/s expected if no folding occurred is 1.0, while a ratio >1.0 is indicative of folding (see text).

Analysis of the relationships among histone acetylation, transcription, and nucleosomal array folding. Higher-order folding of nucleosomal arrays is both repressive to transcription by RNA polymerase III (30, 31) and mediated by the core histone N termini (17, 21, 54). We therefore used the 208-12 model system to investigate whether transcriptional repression due to higher-order folding could be relieved by acetylation. Initially we focused on the transcriptional analysis. Each 5S rDNA repeat of the 208-12 template contains a class III promoter but no termination sequence (Fig. 2A). Functional polymerase III preinitiation complexes assemble on the 5S promoters when incubated in *Xenopus* oocyte nuclear extracts (30, 31). Upon addition of nucleoside triphosphates, RNA polymerase III subsequently initiates transcription at 1 of the 12 promoters and elongates along the template until it either reaches the end of the DNA or is blocked by a repressive structure(s). A distribution of RNA transcripts ranging in size from ~180 to 2,500 bp was produced from both naked 208-12 DNA and unfolded 208-12 nucleosomal arrays (30, 31) (see Fig. 3A). The total transcript level reflects the combined rates of initiation and elongation by RNA polymerase III under the reaction conditions studied. Importantly, for nucleosomal templates, the presence of ≥400-bp transcripts indicates that RNA polymerase III had elongated through two or more nucleosomes during the course of the experiment.

Transcription of underacetylated and highly acetylated 208-12 nucleosomal arrays in transcription buffer containing 50 mM KCl and 5 mM free Mg^{2+} is shown in Fig. 3A. Underacetylated nucleosomal arrays were transcribed very poorly under these high ionic conditions, as observed previously (30, 31). In contrast, substantial increases in RNA transcripts were produced from the highly acetylated arrays under identical reaction conditions (Fig. 3A and B). Controls indicated that the core histone octamers were neither deacetylated nor dissociated from the DNA under the experimental conditions of the transcription experiment (data not shown) (30, 58). Importantly, a naked DNA plasmid containing a single copy of the *Xenopus* 5S rRNA gene added to both reactions was tran-

scribed equivalently (Fig. 3A), indicating that the observed relief of transcriptional repression by acetylation was chromatin specific. Quantitation of the total amount of RNA transcripts indicated a 15- ± 3-fold enhancement of transcription from highly acetylated 12-mer nucleosomal arrays relative to that from underacetylated arrays (Fig. 3C). Under comparable conditions, only an approximately fivefold increase in transcription due to acetylation was seen with 5S dinucleosomes (58). Finally, densitometry results indicated that >70% of the transcripts produced from the highly acetylated nucleosomal arrays ranged from ~400 to 2,500 bp in length (Fig. 3B). These data establish that there is a pronounced enhancement in total read-through transcripts produced from 208-12 nucleosomal arrays when their core histone N termini are highly acetylated.

We next determined the extent of folding of the same underacetylated and highly acetylated samples in transcription buffer with or without salts. Sedimentation velocity experiments using the analytical ultracentrifuge were conducted to assay for higher-order folding. The sedimentation coefficient distributions obtained from this approach (62) provide a precise indication of the extent of folding of the entire population of nucleosomal arrays in a sample under a given set of solution conditions (27, 28, 48). Sedimentation coefficient distributions of underacetylated and highly acetylated 208-12 nucleosomal arrays in transcription buffer lacking salts were nearly homogeneous (data not shown), as is characteristic of mostly saturated preparations of unfolded arrays in low-salt buffers (27, 29, 48). To obtain the percentage increase in sedimentation coefficients due to salt (s^{salts}/s) at each point in the distribution plot, the $s_{20,w}$ obtained in transcription buffer containing 50 mM KCl and 5 mM free Mg^{2+} was divided by the $s_{20,w}$ at the equivalent boundary fraction of unfolded arrays in transcription buffer lacking salts (30, 31). Previous studies have established that the sedimentation coefficients of the unfolded, intermediately folded, and higher-order folded conformational states of a 208-12 nucleosomal array are 29S, 40S, and 55S, respectively (17, 20, 27, 30, 48, 54) (see Fig. 4A). Thus, formation of an intermediately-folded species such as an open helix would yield a 40% increase in the sedimentation coefficient (i.e., $s^{salts}/s = 1.4$), while a s^{salts}/s equal to ~1.9 would indicate formation of a higher-order folded conformation such as a regular or irregular contacting helix (27, 30).

Underacetylated nucleosomal arrays in transcription buffer containing 50 mM KCl and 5 mM free Mg^{2+} yielded s^{salts}/s profiles that ranged from 1.3 to 1.9 (Fig. 3D). This indicates that virtually the entire population of underacetylated arrays were partitioned between the intermediately and higher-order folded conformational states under these conditions. In contrast, highly acetylated nucleosomal arrays exhibited much smaller percentage increases in sedimentation coefficient at all points across the distribution profile (Fig. 3D). These data indicate that an average of 12 acetates per histone octamer was sufficient to substantially disrupt folding of all nucleosomal arrays in the sample. They further show that highly acetylated nucleosomal arrays were incapable of folding beyond an intermediate state, even under the elevated ionic conditions of the transcription experiment. In this regard, the small to intermediate level of folding of the highly acetylated arrays in transcription buffer containing salts ($s^{salts}/s = 1.2$ to 1.45) (Fig. 3D) was virtually identical to that observed for fully trypsinized nucleosomal arrays under similarly high ionic conditions (54). Thus, the residual folding observed in Fig. 3D reflects the intrinsic N-termini-independent folding that occurs in high [Mg^{2+}] more so than the inability of acetylation to cause complete unfolding of nucleosomal arrays (54).

Collectively, the functional and structural data shown in Fig. 3 demonstrate that disruption of higher-order folding of nucleosomal arrays by high levels of acetylation is closely correlated with marked increases in total read-through transcripts produced from 208-12 nucleosomal arrays. In addition, these data have provided the first demonstration that higher-order folding of nucleosomal arrays lacking linker histones can be completely inhibited by acetylation of the core histone N termini. In view of the latter result, we next explored the mechanistic basis of acetylation effects on nucleosomal array condensation.

Identification of multiple acetylation-dependent mechanisms involved in nucleosomal array condensation. Nucleosomal arrays in divalent cation solutions both fold extensively (17, 20, 21, 27, 30, 48, 54) (see Fig. 4A) and also oligomerize through a process that is reversible and cooperative (47, 54). Together these processes are referred to as nucleosomal array condensation. To better understand the molecular basis of acetylation effects on nucleosomal array condensation, we asked the following questions. Is there a critical level of acetylation required to inhibit folding and/or oligomerization? Does acetylation influence folding and oligomerization in the same manner?

To address the first question, sedimentation velocity analyses of underacetylated, moderately acetylated, and highly acetylated nucleosomal arrays were performed in TE buffer containing $MgCl_2$ since nucleosomal arrays do not form higher-order structures in NaCl (21, 22, 27). In the absence of added monovalent cations, underacetylated arrays start to oligomerize above 2 mM $MgCl_2$ (47, 48) (see Fig. 5). Consequently, the optimal conditions for studying higher-order folding of 208-12 nucleosomal arrays are 1 to 2 mM $MgCl_2$ (47, 48). Figure 4B shows the sedimentation coefficient distribution profiles of underacetylated, moderately acetylated, and highly acetylated nucleosomal arrays in 2 mM $MgCl_2$. Recall that the sedimentation coefficients of the unfolded, intermediately folded and higher-order folded states of 208-12 nucleosomal arrays are 29S, 40S, and 55S, respectively. Underacetylated arrays exhibited a characteristic biphasic $s_{20,w}$ distribution ranging from 30 to 55S with a break in the profile at ~40S (Fig. 4B), as observed in previous studies (20, 30, 48, 54). When expressed as s^{salts}/s plots, the distribution ranged from 1.2 to 1.9 (data not shown). Importantly, the $s_{20,w}$ distribution of moderately acetylated arrays was virtually indistinguishable from that of the underacetylated arrays, whereas the sedimentation coefficients of the highly acetylated arrays ranged from only ~25 to 35S (Fig. 4B). These results demonstrate that in 2 mM $MgCl_2$, a level of 6 acetates/nucleosome had no effect on nucleosomal array folding while a level of 12 acetates/nucleosome was able to totally inhibit the formation of the higher-order folded 55S species and substantially disrupt formation of the intermediately folded 40S species. The conclusions of the sedimentation experiments were further tested by using quantitative agarose gel electrophoresis to derive an average R_e from low-percent agarose gels (19, 20). Under these conditions, the R_e yields information about average nucleosomal array shape (19, 20, 28). The R_es of both underacetylated and moderately acetylated arrays derived from dilute gels containing 2 mM $MgCl_2$ were indistinguishable (Fig. 4B), while the R_e of highly acetylated arrays was significantly larger and equal to the R_e of unfolded 208-12 nucleosomal arrays assembled from chicken erythrocyte histone octamers (19, 20). Thus, the quantitative gel analysis independently confirmed the conclusion that the difference between 6 and 12 acetates/histone octamer potently destabilizes nucleosomal array folding. It should be noted that moderately acetylated and highly acetylated 208-12 nucleosomal arrays also could be analyzed by sedimentation velocity in 3 mM $MgCl_2$ (Fig. 4C) due to the fact that acety-

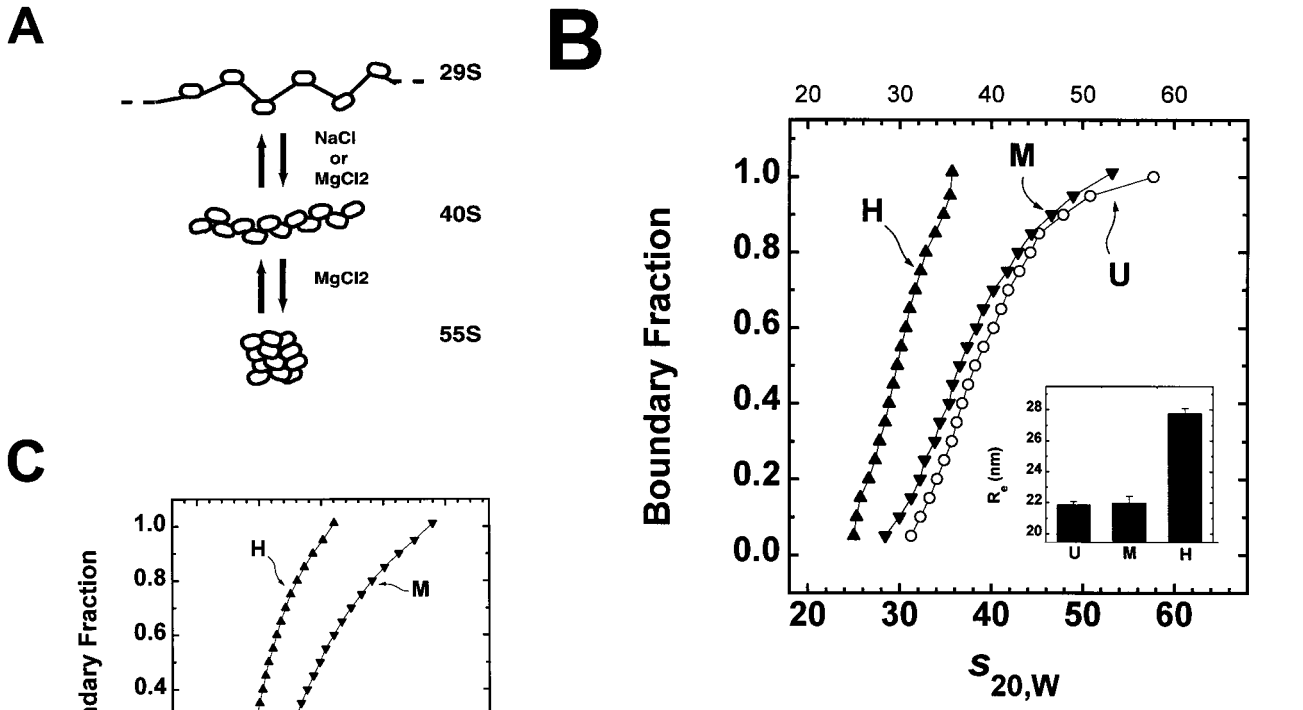

FIG. 4. Comparison of Mg^{2+}-dependent folding of underacetylated, moderately acetylated, and highly acetylated nucleosomal arrays. (A) Illustration of the salt-dependent folding of the 208-12 nucleosomal array as elucidated by sedimentation velocity experiments (27, 48). Shown are schematic representations of array conformations whose extent of compaction would yield the indicated sedimentation coefficients. (B) Sedimentation velocity analysis of underacetylated (U), moderately acetylated (M), and highly acetylated (H), nucleosomal arrays in 2 mM Mg^{2+}. Samples were incubated in TE buffer containing 2 mM free Mg^{2+} for 1 h at room temperature. Sedimentation was performed as described in the legend for panel D of Fig. 3. Shown are the sedimentation coefficient distributions obtained after analysis of the data by the method of van Holde and Weischet (62). The inset shows the R_es of the same samples determined by quantitative agarose gel analysis in E buffer containing 2 mM free Mg^{2+} (see Materials and Methods). The indicated values represent the means ± standard deviations of 18 determinations of the R_e in 0.2 to 0.8% agarose gels ($P_e \geq 200$ nm). At $P_e \geq 200$ nm, the R_es of 208-12 nucleosomal arrays is constant (20, 26). (C) Sedimentation velocity analysis of moderately acetylated (M) and highly acetylated (H) nucleosomal arrays in 3 mM Mg^{2+}. Samples were incubated in TE buffer containing 3 mM free Mg^{2+} for 1 h at room temperature. Sedimentation was performed as described in the legend for panel D of Fig. 3. Shown are the sedimentation coefficient distributions obtained after analysis of the data by the method of van Holde and Weischet (62).

lation increases the amount of $MgCl_2$ required to induce oligomerization (see Fig. 5). Comparison of Fig. 4B and C indicates that sedimentation coefficient profiles of both types of acetylated arrays in 3 mM $MgCl_2$ were increased by several S across the distribution compared to the profiles in 2 mM $MgCl_2$. These results indicate that the equilibrium was shifted toward the more folded states at the higher $MgCl_2$ concentration, consistent with the data in Fig. 3D. Nevertheless, the key conclusions remain unchanged. The increase from an average of 6 to 12 acetates/histone octamer completely inhibits the ability of 208-12 nucleosomal arrays to form higher-order folded species and destabilizes the intermediately folded state as well.

The divalent cation dependence of nucleosomal array condensation is hierarchical; 12-mer arrays first fold and then reversibly oligomerize as the $MgCl_2$ concentration is increased from 0 to 10 mM (18, 47, 48). There is evidence suggesting that oligomerization may be an in vitro manifestation of long-range fiber-fiber interactions found in intact interphase chromosomes (47; reviewed in reference 18). Given that the core histone N termini are absolutely required for oligomerization (47, 54), we next determined whether core histone acetylation influenced oligomerization in the same manner as folding. Cooperative formation of soluble oligomers was indicated by a sharp decrease in the A_{260} of the supernatant after exposure to increasing amounts of salts and subsequent centrifugation in an Eppendorf microcentrifuge (18, 47, 48) (Fig. 5). Sedimentation velocity analyses have demonstrated that only unassociated 12-mer arrays are present in the supernatant after centrifugation, while the oligomers initially sediment at ≥400S and quickly increase in size as the $MgCl_2$ concentration is increased (47). The Mg^{2+} dependence of oligomerization of underacetylated, moderately acetylated, and highly acetylated nucleosomal arrays is shown in Fig. 5. Compared to underacetylated arrays, both the moderately and highly acetylated arrays required a greater amount of $MgCl_2$ to oligomerize: half-maximal oligomerization occurred at ~3.3 mM for underacetylated arrays, at ~4.25 mM for moderately acetylated arrays, and at ~5.5 mM for highly acetylated nucleosomal arrays. These results indicate that in contrast to folding, both moderate and high levels of acetylation influence the ability of nucleosomal arrays to oligomerize.

DISCUSSION

Although a robust correlation between core histone acetylation and transcriptional activation in vivo has been recog-

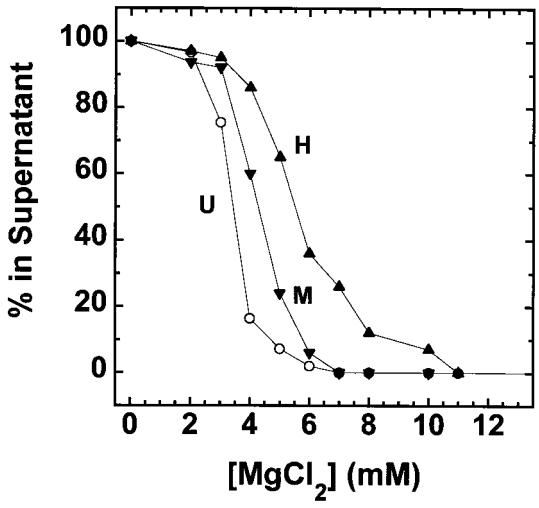

FIG. 5. Mg^{2+}-dependent oligomerization of underacetylated, moderately acetylated, and highly acetylated nucleosomal arrays. Oligomerization was assayed by differential centrifugation as previously described (47, 48). Shown are the percentages of the underacetylated (U), moderately acetylated (M), and highly acetylated (H); samples that remained in the supernatant after exposure to the indicated amounts of $MgCl_2$ for 10 min at room temperature and centrifugation at 16,000 × *g* for 10 min in an Eppendorf microcentrifuge. Each data point represents the mean of three to four determinations.

nized for over two decades (3, 32–34, 45; reviewed in references 55 and 56), the molecular mechanism(s) responsible for enhancement of transcription by acetylation remains to be defined. Particularly little is known about the structure-function relationships governing modulation of higher-order chromatin structure by acetylation. This in part stems from the fact that the effect(s) of acetylation on the stability of highly condensed nucleosomal arrays and chromatin fibers has yet to be completely defined (13, 25, 68). In addition, there is a paucity of experimental systems in which higher-order chromatin structural dynamics and transcriptional activity can be studied concurrently. Finally, virtually all recent in vitro structure-function studies have focused on acetylation effects on mononucleosomes and free histones as opposed to nucleosomal arrays and chromatin (2, 11, 35, 38, 43, 52, 63; reviewed in references 13, 25, and 68). To address this situation, in the present study the mechanistic relationships among histone acetylation, higher-order folding, and transcription were investigated by simultaneously analyzing the extent of folding and transcriptional activity of defined 12-mer nucleosomal array model systems reconstituted from tandemly repeated 5S rDNA and native or acetylated histone octamers. This has allowed us to extend previous observations made with mono- and dinucleosomes to a system that is capable of folding into a complete range of higher-order structures. The in vitro transcription studies have demonstrated a 15-fold enhancement of total 5S rDNA transcription under conditions where acetylation caused the 12-mer nucleosomal arrays to unfold (Fig. 3D). Only an approximately fivefold effect of acetylation was observed with a dinucleosome under the same conditions (58) (Fig. 3C). The structural studies have revealed both that a critical level of acetylation must be reached before higher-order folding of nucleosomal arrays is inhibited and that multiple mechanisms of action are involved in acetylation-dependent disruption of nucleosomal array condensation (Fig. 4 and 5). Together, these results establish a solid molecular link between transcriptional regulation and disruption of higher-order folding by acetylation and further show that there is a complex mechanistic basis for the effects of acetylation on the stability of condensed chromatin.

Histone acetylation functions in concert at multiple levels to regulate the transcriptional activity of nucleosomal arrays. The elegant studies of Crane-Robinson and colleagues have demonstrated that chromatin domains encompassing the entire 33-kb transcription units of several β-globin genes become highly acetylated in vivo 5 to 15 days prior to gene expression but that acetylation per se is not able to induce transcription (32–34). Several lines of evidence suggest that acetylation specifically functions at multiple levels during the subsequent concerted sequence of events that leads to production of full-length RNA transcripts. In the case of the β-globin genes and others like them, large functional chromatin domains must be maintained in a highly acetylated state by a shift in the balance of dynamic histone acetylation-deacetylation (13, 14, 39). Subsequently, the stabilizing effects of linker histones on repressive higher-order chromatin structures (reviewed in references 18, 61, and 67) must be removed. This appears to involve a combination of both linker histone depletion (10, 15, 36, 46) and rearrangement (42, 64). Histone acetylation in part appears to facilitate this process (4, 40). Once these events occur, the requisite transcription factors bind to key regulatory DNA sequences (e.g., promoters and enhancers) and lead to RNA polymerase recruitment and initiation of transcription. There is evidence that acetylation may function at this step by facilitating transcription factor access to nucleosomal DNA (35, 38, 63). In addition, specific histone acetylation by components of the transcriptional machinery (e.g., GCN5p) also are likely to facilitate one or more steps in the initiation process through mechanisms that remain to be established. Importantly, because linker histone depletion-rearrangement is insufficient to remove the inhibitory effects of higher-order nucleosomal array folding on both transcription initiation and elongation (30, 31), disruption of array folding by acetylation in principle should allow eukaryotic RNA polymerases to more efficiently initiate transcription and subsequently elongate through entire large chromatin domains. Finally, there is also evidence that acetylation facilitates polymerase processivity through the individual nucleosomes of the nucleosomal array (58). Taken together, all available evidence suggests that acetylation of the core histone N termini has essential structural and functional consequences at all levels from the higher-order chromosomal domain to the nucleosome and that the multiple effects of acetylation function in concert to help allow the transcriptional machinery to efficiently transcribe through long stretches of chromatin.

Complexity of acetylation involvement in nucleosomal array condensation. Characterization of the folding properties of differentially acetylated nucleosomal arrays has allowed us to determine whether acetylation of the N termini can mimic some or all of the structural consequences of complete tail domain removal. Recent analyses of selectively trypsinized nucleosomal arrays have revealed that the N termini are absolutely required for both higher-order folding and cooperative oligomerization in 2 to 3 mM $MgCl_2$ (17, 21, 54). At higher $MgCl_2$ concentrations, trypsinized nucleosomal arrays are able to form an ~40S intermediately folded species but cannot form the 55S higher-order folded conformation (54). Interestingly, the Mg^{2+}-dependent folding behavior of highly acetylated nucleosomal arrays (Fig. 3D and 4) is virtually the same as that of fully trypsinized nucleosomal arrays lacking all their N termini (54). Thus, an average level of 12 acetates/octamer essentially is as effective at inhibiting nucleosomal array folding as is complete proteolytic removal of the N termini. This is not the

case for oligomerization, however. Increasing levels of acetylation of the N termini partially disrupt oligomerization, as evidenced by the requirement for increased amounts of $MgCl_2$, but acetylation does not completely abolish this structural transition (Fig. 5). In contrast, nucleosomal arrays lacking all their N termini are unable to oligomerize under any salt conditions (47, 54). Thus, the acetylation results support the conclusion that folding and oligomerization are mediated by distinct mechanistic functions of the N termini (47, 54).

Studies of selectively trypsinized nucleosomal arrays also led us to propose that the role of the core histone N termini in higher-order folding involves protein-protein interactions while the interactions of the N termini that mediate oligomerization involve a separate mechanism that consists of both protein-protein and protein-DNA components (54). It was further observed that contributions from the N termini of both the H3-H4 and H2A-H2B pairs were required to achieve higher-order folding, whereas the N termini of H3-H4 or H2A-H2B pairs alone could mediate oligomerization (54). Our studies of differentially acetylated nucleosomal arrays both support and extend many of the conclusions derived from the proteolysis studies. The observation that an average of 12 but not 6 acetates/octamer inhibited higher-order folding under all ionic strengths tested (Fig. 3D and 4) is inconsistent with a simple charge neutralization-based mechanism of N termini function in higher-order folding. This is further supported by the fact that higher-order folding is inhibited under conditions where only 12 of the ~100 positive charges in the N termini of each octamer are neutralized by acetylation. A more likely possibility is that acetylation disrupts secondary structure within the N termini essential for the internucleosomal interactions in *cis* and *trans* that mediate condensation. In this regard, it is known that lysine acetylation destabilizes α-helices (7, 69) and that the H3-H4 N termini contain ~50% α-helical content when complexed with nucleosomal DNA (6; also see reference 26). Recall that the difference between moderately and highly acetylated nucleosomal arrays is an enrichment in di-, tri-, and tetraacetylated H4; triacetylated H2B; and tri- and tetraacetylated H3 (Table 1). Thus, together with the results obtained from the selective proteolysis experiments (54), the simplest explanation for the threshold effect of acetylation on higher-order folding is that a critical level of bulk acetylation is necessary to achieve acetylation of the specific lysine residues in the H4, H3, and H2B N termini that are responsible for disrupting the structural motif(s) necessary for higher-order folding. Interestingly, several transcription-relevant histone acetyltransferases (e.g., GCN5p) recently have been shown to exhibit high substrate specificity in vitro, with different enzymes preferring specific lysine residues in each of the core histone N termini (reviewed in reference 13). Thus, it is possible that at least one of the in vivo functions of specific histone acetylation may be to modify the key lysines that control repressive higher-order nucleosomal array folding. In contrast to the mechanism of folding, the partial disruptive effect of acetylation on oligomerization appears to be electrostatic in nature as evidenced by the sequential need for more Mg^{2+} in response to sequential increases in the bulk level of histone acetylation (Fig. 5). In this case, acetylation only appears to influence the electrostatic component of N-termini-mediated oligomerization. Ultimately, the differential effects of acetylation on folding and oligomerization appear to originate directly from the multiple molecular mechanisms through which the core histone N termini mediate chromatin condensation.

ACKNOWLEDGMENTS

We thank James Davie for technical advice relating to isolation of acetylated histone octamers.

Takashi Sera is a JSPS research fellow in Biomedical and Behavioral Research at the N.I.H. This work was supported by National Institutes of Health grant GM45916 to J.C.H.

REFERENCES

1. **Allan, J., N. Harborne, D. C. Rau, and H. Gould.** 1982. Participation of core histone "tails" in the stabilization of the chromatin solenoid. J. Cell Biol. **93:**285–297.
2. **Alland, L., R. Muhle, H. Hou, Jr., J. Potes, L. Chin, N. Schreiber-Agus, and R. A. DePinho.** 1997. Role for N-CoR and histone deacetylase in Sin3-mediated transcriptional repression. Nature **387:**49–55.
3. **Allfrey, V., R. M. Faulkner, and A. E. Mirsky.** 1964. Acetylation and methylation of histones and their possible role in the regulation of RNA synthesis. Proc. Natl. Acad. Sci. USA **51:**786–794.
4. **Annunziato, A. T., L. L. Frado, R. L. Seale, and C. L. Woodcock.** 1988. Treatment with sodium butyrate inhibits the complete condensation of interphase chromatin. Chromosoma **96:**132–138.
5. **Ausio, J., and K. E. van Holde.** 1986. Histone hyperacetylation: its effects on nucleosome conformation and stability. Biochemistry **25:**1421–1428.
6. **Banéres, J.-L., A. Martin, and J. Parello.** 1997. The N tails of histones H3 and H4 adopt a highly structured conformation in the nucleosome. J. Mol. Biol. **273:**503–508.
7. **Batra, P. P., M. A. Roebuck, and D. Uetrecht.** 1990. Effect of lysine modification on the secondary structure of ovalbumin. J. Prot. Chem. **9:**37–44.
8. **Bednar, J., R. A. Horowitz, J. Dubochet, and C. L. Woodcock.** 1995. Chromatin conformation and salt-induced compaction: three-dimensional structural information from cryoelectron microscopy. J. Cell Biol. **131:**1365–1376.
9. **Birkenmeier, E. H., D. D. Brown, and E. Jordan.** 1978. A nuclear extract of Xenopus laevis oocytes that accurately transcribes 5S RNA genes. Cell **15:**1077–1086.
10. **Bresnick, E. H., S. John, and G. L. Hager.** 1991. Histone hyperacetylation does not alter the positioning or stability of phased nucleosomes on the mouse mammary tumor virus long terminal repeat. Biochemistry **30:**3490–3497.
11. **Brownell, J. E., J. Zhou, T. Ranalli, R. Kobayashi, D. G. Edmondson, S. Y. Roth, and C. D. Allis.** 1996. Tetrahymena histone acetyltransferase A: a homolog to yeast Gcn5p linking histone acetylation to gene activation. Cell **84:**843–851.
12. **Davie, J. R.** 1982. Two-dimensional gel systems for rapid histone analysis for use in minislab polyacrylamide gel electrophoresis. Anal. Biochem. **120:**276–281.
13. **Davie, J. R.** Covalent modifications of histones: expression from chromatin templates. Curr. Opin. Gen. Devel., in press.
14. **Davie, J. R., and M. J. Hendzel.** 1994. Multiple functions of dynamic histone acetylation. J. Cell Biochem. **55:**98–105.
15. **Dedon, P. C., J. A. Soults, C. D. Allis, and M. A. Gorovsky.** 1991. Formaldehyde cross-linking and immunoprecipitation demonstrate developmental changes in H1 association with transcriptionally active genes. Mol. Cell. Biol. **11:**1729–1733.
16. **Dong, F., J. C. Hansen, and K. E. van Holde.** 1990. DNA and protein determinants of nucleosome positioning on sea urchin 5S rRNA gene sequences in vitro. Proc. Natl. Acad. Sci. USA **87:**5724–5728.
17. **Fletcher, T. M., and J. C. Hansen.** 1995. Core histone tail domains mediate oligonucleosome folding and nucleosomal DNA organization through distinct molecular mechanisms. J. Biol. Chem. **270:**25359–25362.
18. **Fletcher, T. M., and J. C. Hansen.** 1996. The nucleosomal array: structure/function relationships. Crit. Rev. Eukaryot. Gene Exp. **6:**149–188.
19. **Fletcher, T. M., U. Krishnan, P. Serwer, and J. C. Hansen.** 1994. Quantitative agarose gel electrophoresis of chromatin: nucleosome-dependent changes in charge, shape, and deformability at low ionic strength. Biochemistry **33:**2226–2233.
20. **Fletcher, T. M., P. Serwer, and J. C. Hansen.** 1994. Quantitative analysis of macromolecular conformational changes using agarose gel electrophoresis: application to chromatin folding. Biochemistry **33:**10859–10863.
21. **Garcia-Ramirez, M., F. Dong, and J. Ausio.** 1992. Role of the histone "tails" in the folding of oligonucleosomes depleted of histone H1. J. Biol. Chem. **267:**19587–19595.
22. **Garcia-Ramirez, M., C. Rocchini, and J. Ausio.** 1995. Modulation of chromatin folding by histone acetylation. J. Biol. Chem. **270:**17923–17928.
23. **Georgel, P., B. Demeler, C. Terpening, M. R. Paule, and K. E. van Holde.** 1993. Binding of the RNA polymerase I transcription complex to its promoter can modify positioning of downstream nucleosomes assembled in vitro. J. Biol. Chem. **268:**1947–1954.
24. **Griess, G. A., E. T. Moreno, R. A. Easom, and P. Serwer.** 1989. The sieving of spheres during agarose gel electrophoresis: quantitation and modeling. Biopolymers **28:**1475–1484.
25. **Grunstein, M.** 1997. Histone acetylation in chromatin structure and transcription. Nature **389:**349–352.

26. **Hansen, J. C.** 1997. The core histone amino-termini: combinatorial interaction domains that link chromatin structure with function. Chemtracts Biochem. Mol. Biol. **10:**56–69.
27. **Hansen, J. C., J. Ausio, V. H. Stanik, and K. E. van Holde.** 1989. Homogeneous reconstituted oligonucleosomes, evidence for salt-dependent folding in the absence of histone H1. Biochemistry **28:**9129–9136.
28. **Hansen, J. C., J. I. Kreider, B. Demeler, and T. M. Fletcher.** 1997. Analytical ultracentrifugation and agarose gel electrophoresis as tools for studying chromatin folding in solution. Methods Comp. Methods Enzymol. **12:**62–72.
29. **Hansen, J. C., and D. Lohr.** 1993. Assembly and structural properties of subsaturated chromatin arrays. J. Biol. Chem. **268:**5840–5848.
30. **Hansen, J. C., and A. P. Wolffe.** 1992. Influence of chromatin folding on transcription initiation and elongation by RNA polymerase III. Biochemistry **31:**7977–7988.
31. **Hansen, J. C., and A. P. Wolffe.** 1994. A role for histones H2A/H2B in chromatin folding and transcriptional repression. Proc. Natl. Acad. Sci. USA **91:**2339–2343.
32. **Hebbes, T. R., A. L. Clayton, A. W. Thorne, and C. Crane-Robinson.** 1994. Core histone hyperacetylation co-maps with generalized DNase I sensitivity in the chicken beta-globin chromosomal domain. EMBO J. **13:**1823–1830.
33. **Hebbes, T. R., A. W. Thorne, A. L. Clayton, and C. Crane-Robinson.** 1992. Histone acetylation and globin gene switching. Nucleic Acids Res. **20:**1017–1022.
34. **Hebbes, T. R., A. W. Thorne, and C. Crane-Robinson.** 1988. A direct link between core histone acetylation and transcriptionally active chromatin. EMBO J. **7:**1395–1402.
35. **Howe, L., and J. Ausio.** 1998. Nucleosome translational position, not histone acetylation, determines TFIIIA binding to nucleosomal *Xenopus laevis* 5S rRNA genes. Mol. Cell. Biol. **18:**1156–1162.
36. **Kamakaka, R. T., and J. O. Thomas.** 1990. Chromatin structure of transcriptionally competent and repressed genes. EMBO J. **9:**3997–4006.
37. **Laemmli, U. K.** 1970. Cleavage of structural proteins during the assembly of the head of bacteriophage T4. Nature **227:**680–685.
38. **Lee, D. Y., J. J. Hayes, D. Pruss, and A. P. Wolffe.** 1993. A positive role for histone acetylation in transcription factor access to nucleosomal DNA. Cell **72:**73–84.
39. **Loidl, P.** 1994. Histone acetylation: facts and questions. Chromosoma **103:**441–449.
40. **McGhee, J. D., J. M. Nickol, G. Felsenfeld, and D. C. Rau.** 1983. Histone hyperacetylation has little effect on the higher order folding of chromatin. Nucleic Acids Res. **11:**4065–4075.
41. **Meersseman, G., S. Pennings, and E. M. Bradbury.** 1991. Chromatosome positioning on assembled long chromatin. Linker histones affect nucleosome placement on 5S rDNA. J. Mol. Biol. **220:**89–100.
42. **Nacheeva, G. A., D. Y. Guschin, O. V. Preobrazhenskaya, V. L. Karpov, K. K. Elbradise, and A. D. Mirzabekov.** 1989. Change in the pattern of histone binding to DNA upon transcriptional activation. Cell **58:**27–36.
43. **Ogryzko, V. V., R. L. Schiltz, V. Russanova, B. H. Howard, and Y. Nakatani.** 1996. The transcriptional coactivators p300 and CBP are histone acetyltransferases. Cell **87:**953–959.
44. **Owen-Hughes, T., and J. L. Workman.** 1994. Experimental analysis of chromatin function in transcription control. Crit. Rev. Eukaryot. Gene Exp. **4:**403–441.
45. **Pogo, B. G., V. G. Allfrey, and A. E. Mirsky.** 1966. RNA synthesis and histone acetylation during the course of gene activation in lymphocytes. Proc. Natl. Acad. Sci. USA **55:**805–812.
46. **Postnikov, Y. V., V. V. Shick, A. V. Belyavsky, K. R. Khrapko, K. L. Brodolin, T. A. Nikolskaya, and A. D. Mirzabekov.** 1991. Distribution of high mobility group proteins 1/2, E and 14/17 and linker histones H1 and H5 on transcribed and non-transcribed regions of chicken erythrocyte chromatin. Nucleic Acids Res. **19:**717–725.
47. **Schwarz, P. M., A. Felthauser, T. M. Fletcher, and J. C. Hansen.** 1996. Reversible oligonucleosome self-association: dependence on divalent cations and core histone tail domains. Biochemistry **35:**4009–4015.
48. **Schwarz, P. M., and J. C. Hansen.** 1994. Formation and stability of higher order chromatin structures. Contributions of the histone octamer. J. Biol. Chem. **269:**16284–16289.
49. **Shaw, O. J.** 1969. Electrophoresis. Academic Press, London, United Kingdom.
50. **Simon, R. H., and G. Felsenfeld.** 1979. A new procedure for purifying histone pairs H2A+H2B and H3+H4 from chromatin using hydroxylapatite. Nucleic Acids Res. **6:**689–696.
51. **Simpson, R. T., F. Thoma, and J. M. Brubaker.** 1985. Chromatin reconstituted from tandemly repeated cloned DNA fragments and core histones: a model system for study of higher order structure. Cell **42:**799–808.
52. **Taunton, J., C. A. Hassig, and S. L. Schreiber.** 1996. A mammalian histone deacetylase related to the yeast transcriptional regulator Rpd3p. Science **272:**408–411.
53. **Thorne, A. W., D. Kmiciek, K. Mitchelson, P. Sautiere, and C. Crane-Robinson.** 1990. Patterns of histone acetylation. Eur. J. Biochem. **193:**701–713.
54. **Tse, C., and J. C. Hansen.** 1997. Hybrid trypsinized nucleosomal arrays: identification of multiple functional roles of the H2A/H2B and H3/H4 N-termini in chromatin fiber compaction. Biochemistry **36:**11381–11388.
55. **Turner, B. M.** 1991. Histone acetylation and control of gene expression. J. Cell Sci. **99:**13–20.
56. **Turner, B. M.** 1993. Decoding the nucleosome. Cell **75:**5–8.
57. **Turner, B. M., A. J. Birley, and J. Lavender.** 1992. Histone H4 isoforms acetylated at specific lysine residues define individual chromosomes and chromatin domains in Drosophila polytene nuclei. Cell **69:**375–384.
58. **Ura, K., H. Kurumizaka, S. Dimitrov, G. Almouzni, and A. P. Wolffe.** 1997. Histone acetylation: influence on transcription, nucleosome mobility and positioning, and linker histone-dependent transcriptional repression. EMBO J. **16:**2096–2107.
59. **Usachenko, S. I., S. G. Bavykin, I. M. Gavin, and E. M. Bradbury.** 1994. Rearrangement of the histone H2A C-terminal domain in the nucleosome. Proc. Natl. Acad. Sci. USA **91:**6845–6849.
60. **van Holde, K., and J. Zlatanova.** 1996. What determines the folding of the chromatin fiber? Proc. Natl. Acad. Sci. USA **93:**10548–10555.
61. **van Holde, K. E.** 1988. Chromatin. Springer-Verlag, New York, N.Y.
62. **van Holde, K. E., and W. O. Weischet.** 1978. Boundary analysis of sedimentation—velocity experiments with monodisperse and paucidisperse solutes. Biopolymers **17:**1387–1403.
63. **Vettese-Dadey, M., P. A. Grant, T. R. Hebbes, C. Crane-Robinson, C. D. Allis, and J. L. Workman.** 1996. Acetylation of histone H4 plays a primary role in enhancing transcription factor binding to nucleosomal DNA in vitro. EMBO J. **15:**2508–2518.
64. **Weintraub, H.** 1985. Assembly and propagation of repressed and derepressed chromosomal states. Cell **42:**705–711.
65. **West, M. H., and W. M. Bonner.** 1980. Histone H2A, a heteromorphous family of eight protein species. Biochemistry **19:**3238–3245.
66. **Wolffe, A. P.** 1989. Transcriptional activation of Xenopus class III genes in chromatin isolated from sperm and somatic nuclei. Nucleic Acids Res. **17:**767–780.
67. **Wolffe, A. P.** 1995. Chromatin: structure and function. Academic Press, New York, N.Y.
68. **Wolffe, A. P., J. Wong, and D. Pruss.** 1997. Activators and repressors: making use of chromatin to regulate transcription. Genes Cells **2:**291–302.
69. **Xu, X., L. G. Cooper, P. J. Dimario, and J. W. Nelson.** 1994. Helix formation in model peptides based on nucleolin TPAKK motifs. Biopolymers **35:**93–102.
70. **Yao, J., P. T. Lowary, and J. Widom.** 1990. Direct detection of linker DNA bending in defined-length oligomers of chromatin. Proc. Natl. Acad. Sci. USA **87:**7603–7607.
71. **Yao, J., P. T. Lowary, and J. Widom.** 1991. Linker DNA bending induced by the core histones of chromatin. Biochemistry **30:**8408–8414.